Shunt Hybrid Power Filter and Thyristor-Controlled Reactor based Power Quality Improvement Using Fuzzy Logic Controller

Kotte.deepthi kumari

M-tech Student Scholar Department of Electrical & Electronics Engineering, Nova Engineering College, Jupudi, Ibrahimpatnam; Krishna (Dt); A.P, India

D. kiran kumar

Assistant Professor Department of Electrical & Electronics Engineering, Nova Engineering College, Jupudi, Ibrahimpatnam; Krishna (Dt); A.P, India

Abstract –
Any electrical power system consists of wide range of electrical and power electronic equipment in commercial and industrial applications. The quality of the power is effected by many factors like harmonic contamination, due to the increment of non-linear loads, like large thyristor power converters, voltage and current flickering due to arc in arc furnaces and swell due to the switching of the loads etc. The uncontrolled ac-dc converter suffers from operating problems of poor power factor, injection of harmonics into the ac mains, variations in dc link voltage of input ac supply, equipment overheating due to harmonic current absorption, voltage distortion due to the voltage drop caused by harmonic currents flowing through system impedances, interference on telephone and communication line etc. A Fuzzy logic controller was used to control the TCR. A nonlinear control of APF was developed for current tracking and voltage regulation. The latter is based on a decoupled control strategy, which considers that the controlled system may be divided into an inner fast loop and an outer slow one. Thus, an exact linearization control was applied to the inner loop, and a nonlinear feedback control law was used for the outer voltage loop. The simulation results are found to be quite satisfactory to mitigate harmonic distortions and reactive power compensation.

Index Terms—Harmonic Suppression; Hybrid Power filter; Modeling; Hybrid Power filter And Thyristor-Controller Dreactor (SHPF-TCR Compensator); Fuzzy Logic Controller

I. INTRODUCTION

Global competition is ballooning, forcing companies to seek value and automate processes where ever possible. Computer technology is increasingly used to accomplish these goals, which means more compute power is required [1]. The growing use of non-linear and time varying loads has led to distortion of voltage and current wave forms and increased in reactive power demand in AC mains. Harmonic distortion is known to be source of several problems such as increased power losses, excessive heating of rotating machines, audible noise and incorrect operation of sensitive loads etc [2]. To design a more cost-effective power distribution system for modern computer systems, this paper defines mitigation technique using SHPF-TCR, discusses options that might be recommended to control Shunt Active Filter [1],[9].

However, the costs of active filters are relatively high for large-scale system and require high power converter ratings [9], [10]. Hybrid filters effectively soften the problems of the passive filter and an active filter solution and provide cost-effective harmonic compensation, particularly for high-power nonlinear loads [11]. Many control techniques such as instantaneous reactive power theory, synchronous rotating reference frame, sliding-mode controllers, neural network techniques, nonlinear control [12], feed forward control [13], Lyapunov-function-based control [14], etc., have been used to improve the performance of the active and hybrid filters.

Several filter topologies for compensating harmonics and reactive power have been reported in the literature. In, a multi converter conditioner topology formed by an active conditioner operating in parallel with a hybrid conditioner has been proposed.

A control technique is proposed to improve the dynamic response and decrease the steady-state error of the TCR. It consists of a PI controller and a lookup table to extract the required firing angle to compensate a reactive power consumed by the load. A nonlinear control of SHPF is developed for current tracking and voltage regulation purposes. It is based on a decoupled control strategy, which considers that the controlled system may be divided into an inner fast loop and an outer slow one. The currents injected by the SHPF are controlled in the synchronous orthogonal dq frame using a decoupled feedback linearization control method. The dc bus voltage is regulated using an output feedback linearization control. The SHPF can maintain the low level of dc bus voltage at a stable value below 50 V. The proposed nonlinear control scheme has been simulated and validated experimentally to compute the performance of the proposed SHPF-TCR compensator with harmonic and reactive power compensation and analysis through the total harmonic distortion (THD) of the source and the load current. The proposed methodology is tested for a wide range of loads as discussed further. Simulation results show that the proposed topology is suitable for harmonic suppression and reactive compensation.

The current reference circuit generates the reference currents required to compensate the load current harmonics and reactive power, and also try to maintain constant the dc voltage across the capacitor [3]. In this paper, a new combination of a shunt hybrid power filter (SHPF) and a TCR (SHPF-TCR compensator) is proposed to suppress current harmonics and compensate the reactive power generated from the load. The hybrid filter consists of a series connection of a small-rated active filter and a fifth tuned LC passive filter. In the proposed topology, the major part of the compensation is supported by the passive filter and the TCR while the APF is meant to improve the filtering characteristics and damps the resonance, which can occur between the passive filter, the TCR, and the source impedance. The shunt APF when used alone suffers from the high kilo volt ampere rating of the inverter, which requires a lot of energy stored at high dc-link voltage. On the other hand, as published by some authors, the standard hybrid power filter is unable to compensate the reactive power because of the behaviour of the passive filter.

Because of these merits, the presented combined topology is very appropriate in compensating reactive power and eliminating harmonic currents in power system. These works study the compensation principle and different control strategies used here are based on PI/FUZZY controller of the shunt and TCR active filter in detail. The control strategies are modelled using MATLAB/SIMULINK. The performance is also observed under influence of utility side disturbances such as harmonics, flicker and spikes with Non-Linear and Reactive Loads. The simulation results are listed in comparison of different control strategies and for the verification of results.

III. MODELING AND CONTROL STRATEGY

A. Modeling of SHPF

The system equations are first elaborated in 123 reference frame. Using Kirchhoff's voltage law, one can write

$$v_{s1} = L_{PF}\frac{di_{c1}}{dt} + R_{PF}i_{c1} + v_{CPF1} + v_{1M} + v_{MN}$$

$$v_{s2} = L_{PF}\frac{di_{c2}}{dt} + R_{PF}i_{c2} + v_{CPF2} + v_{2M} + v_{MN}$$

$$v_{s3} = L_{PF}\frac{di_{c3}}{dt} + R_{PF}i_{c3} + v_{CPF3} + v_{3M} + v_{MN}$$

$$v_{CPF1} = L_T\frac{di_{c1}}{dt} - C_{PF}L_T\frac{d^2v_{CPF1}}{dt^2}$$

$$v_{CPF2} = L_T\frac{di_{c2}}{dt} - C_{PF}L_T\frac{d^2v_{CPF2}}{dt^2}$$

$$v_{CPF3} = L_T\frac{di_{c3}}{dt} - C_{PF}L_T\frac{d^2v_{CPF3}}{dt^2}$$

$$\frac{dv_{dc}}{dt} = \frac{1}{C_{dc}}i_{dc}.$$

$$(1)$$

The switching function ck of the kth leg of the converter (for $k = 1, 2, 3$) is defined as

$$c_k = \begin{cases} 1, & \text{if } S_k \text{ is On and } S'_k \text{ is Off} \\ 0, & \text{if } S_k \text{ is Off and } S'_k \text{ is On.} \end{cases} \quad (2)$$

A switching state function d_{nk} is defined as

$$d_{nk} = \left(c_k - \frac{1}{3} \sum_{m=1}^{3} c_m \right)_n \quad (3)$$

Moreover, the absence of the zero sequence in the ac currents and voltages and in the $[d_{nk}]$ functions leads to the following transformed model in the three-phase coordinates [15]:

$$L_{PF} \frac{di_{c1}}{dt} = -R_{PF}i_{c1} - d_{n1}v_{dc} - v_{CPF1} + v_{s1}$$

$$L_{PF} \frac{di_{c2}}{dt} = -R_{PF}i_{c2} - d_{n2}v_{dc} - v_{CPF2} + v_{s2}$$

$$L_{PF} \frac{di_{c3}}{dt} = -R_{PF}i_{c3} - d_{n3}v_{dc} - v_{CPF3} + v_{s3}$$

$$C_{dc} \frac{dv_{dc}}{dt} + \frac{v_{dc}}{R_{dc}} = d_{n1}i_{c1} + d_{n2}i_{c2} + d_{n3}i_{c3}. \quad (4)$$
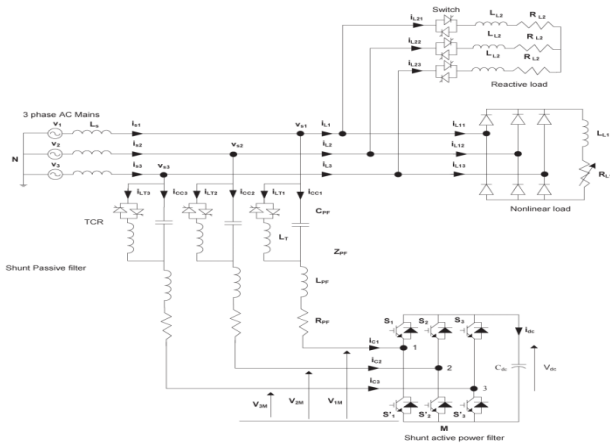
Fig.1. Basic circuit of the proposed SHPF-TCR compensator.

The system of (4) is transformed into the synchronous orthogonal frame using the following general transformation matrix:

$$C_{dq}^{123} = \sqrt{\frac{2}{3}} \begin{bmatrix} \cos\theta & \cos(\theta - 2\pi/3) & \cos(\theta - 4\pi/3) \\ -\sin\theta & -\sin(\theta - 2\pi/3) & -\sin(\theta - 4\pi/3) \end{bmatrix} \quad (5)$$

Where $\theta = \omega t$ and the following equalities hold:

$$C_{123}^{dq} = (C_{dq}^{123})^{-1} = (C_{dq}^{123})^T$$

Then, by applying dq transformation, the state space model of the system in the synchronous reference frame

This model is nonlinear because of the existence of multiplication terms between the state variables {id, iq, Vdc} and the switching state function {dnd, dnq}. However, the model is time invariant during a given switching state.

Furthermore, the principle of operation of the SHPF requires that the three state variables have to be controlled independently. The interaction between the inner current loop and the outer dc bus voltage loop can be avoided by adequately separating their respective dynamics.

B. Harmonic Current Control

A fast inner current loop, and a slow outer dc voltage loop, is adopted. The first two equations in the model can be written as shown in the Appendix by (27). Note that the first and the second time derivative TCR capacitor voltages have no significant negative impact on the performance of the proposed control technique because their coefficients are too low. Consequently, they can practically be ignored. Define the equivalent inputs by (28) as given in the Appendix.
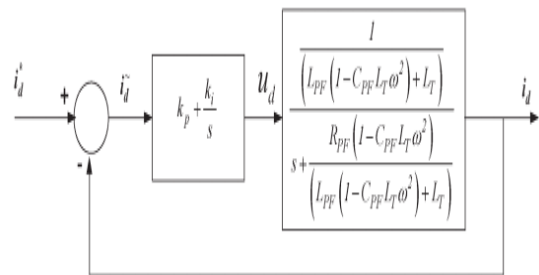
Fig.2. Inner control loop of the current i_d.

Thus, with this transformation, the decoupled dynamics of the current tracking is obtained. The currents id and iq can be controlled independently. Furthermore, by using proportional integral compensation, a fast dynamic response and zero steady-state errors can be achieved. The expressions of the tracking controllers are

$$u_d = \left(L_{PF}(1 - C_{PF}L_T\omega^2) + L_T \right) \frac{di_d}{dt} + R_{PF}(1 - C_{PF}L_T\omega^2)i_d$$

$$= k_p \tilde{i}_d + k_i \int \tilde{i}_d dt$$

$$u_q = \left(L_{PF}(1 - C_{PF}L_T\omega^2) + L_T \right) \frac{di_q}{dt} + R_{PF}(1 - C_{PF}L_T\omega^2)i_q$$

$$= k_p \tilde{i}_q + k_i \int \tilde{i}_q dt$$

The transfer function of the proportional–integral controllers is given as

$$G_{i1}(s) = \frac{U_d(s)}{\tilde{i}_d(s)} = k_{p1} + \frac{k_{i1}}{s}$$

$$G_{i2}(s) = \frac{U_q(s)}{\tilde{i}_q(s)} = k_{p2} + \frac{k_{i2}}{s} \tag{7}$$

The inner control loop of the current i_d is shown in Fig.2.The closed-loop transfer functions of the current loops are

$$\frac{I_d(s)}{I_d^*(s)} = \frac{k_{p1}}{A} \frac{\left(s + \frac{k_{i1}}{k_{p1}}\right)}{s^2 + \left(\frac{B+k_{p1}}{A}\right)s + k_{i1}}$$

$$\frac{I_q(s)}{I_q^*(s)} = \frac{k_{p2}}{A} \frac{\left(s + \frac{k_{i2}}{k_{p2}}\right)}{s^2 + \left(\frac{B+k_{p2}}{A}\right)s + k_{i2}} \tag{8}$$

The closed-loop transfer functions of the current loops have the following form:

$$\frac{I_d(s)}{I_d^*(s)} = 2\zeta\omega_{ni} \frac{s + \frac{\omega_{ni}}{2\zeta}}{s^2 + 2\zeta\omega_{ni}s + \omega_{ni}^2}$$

Where ω_{ni} is the outer loop natural angular frequency and ζ is the damping factor. For the optimal value of the damping factor $\zeta = \sqrt{2}/2$, the theoretical overshoot is 20.79%. The following design relations can be derived:

$$k_{p1} = k_{p2} = 2\zeta\omega_{ni}\left(L_{PF}\left(1 - C_{PF}L_T\omega^2\right) + L_T\right) - R_{PF}\left(1 - C_{PF}L_T\omega^2\right)$$

$$k_{i1} = k_{i2} = \left(L_{PF}\left(1 - C_{PF}L_T\omega^2\right) + L_T\right)\omega_{ni}^2$$

The control law is given in the Appendix by (29) and (30). Note that the inputs qnd and $q$nq consist of a nonlinearity cancellation part and a linear decoupling compensation part.

C. DC Bus Voltage Regulation
In order to maintain the dc bus voltage level at a desired value, acting on iq can compensate the losses through the hybrid power filter components. The output of the controller is added to the q-component current reference iq as shown in Fig. 3. The third equation in the model (6) is rewritten

$$C_{dc}\frac{dv_{dc}}{dt} + \frac{v_{dc}}{R_{dc}} = d_{nq}i_q \tag{10}$$

The three-phase filter currents are given by

$$\begin{bmatrix} i_{c1} \\ i_{c2} \\ i_{c3} \end{bmatrix} = \sqrt{\frac{2}{3}}i_q \begin{bmatrix} -\sin\theta \\ -\sin\left(\theta - \frac{2\pi}{3}\right) \\ -\sin\left(\theta - \frac{2\pi}{3}\right) \end{bmatrix} \tag{11}$$

The fundamental filter rms current Ic is

$$I_c = \frac{i_q}{\sqrt{3}}. \tag{12}$$

The q-axis active filter voltage vMq is expressed as

$$v_{Mq} = q_{nq}v_{dc} = -Z_{PF1}i_{q1}^* \tag{13}$$

Where ZPF1 is the impedance of the passive filter at 60 Hz and $i*q$1 is a dc component.
An equivalent input $u$dc is defined as

$$u_{dc} = q_{nq}i_q \tag{14}$$

The control effort of the dc voltage loop is deduced

$$i_{q1}^* = \frac{v_{dc}}{-Z_{PF1}i_q}u_{dc}. \tag{15}$$

The dc component will force the SHPF-TCR compensator to generate or to draw a current at the fundamental frequency.
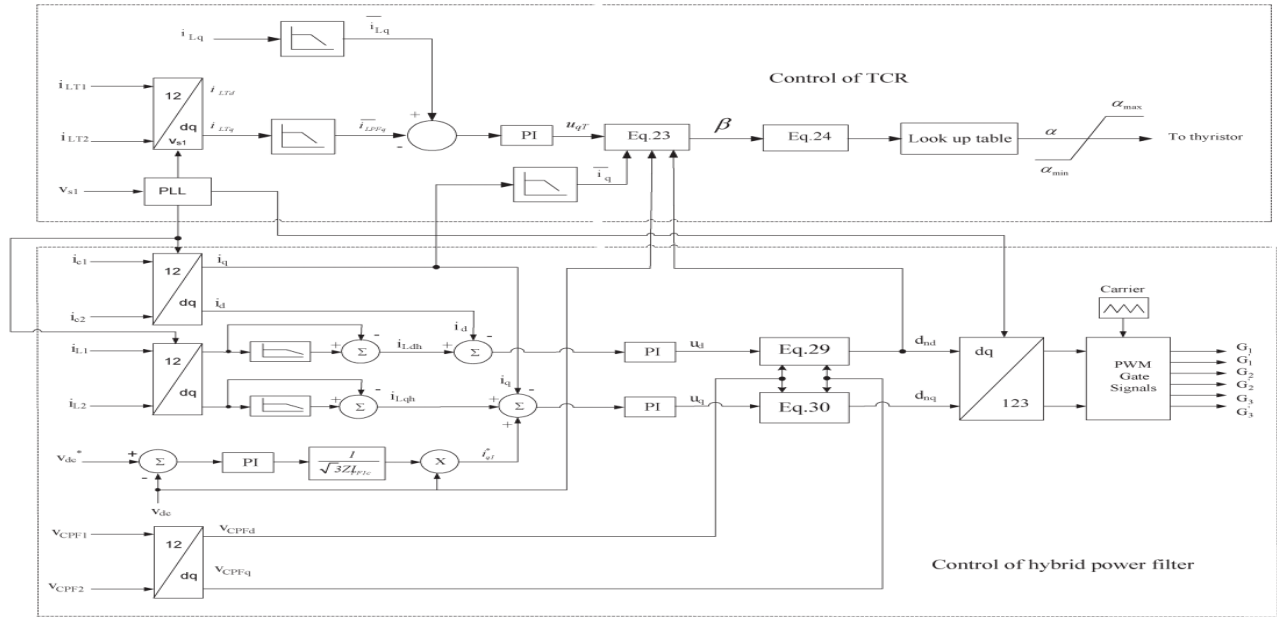
Fig.3.Control scheme of the proposed SHPF-TCR compensator.

The response of the dc bus voltage loop is a second-order transfer function and has the following form:

$$\frac{V_{\mathrm{dc}}(s)}{V_{\mathrm{dc}}^*(s)} = 2\zeta\omega_{\mathrm{nv}}\frac{s + \frac{\omega_{\mathrm{nv}}}{2\zeta}}{s^2 + 2\zeta\omega_{\mathrm{nv}}s + \omega_{\mathrm{nv}}^2}$$

The closed-loop transfer function of dc bus voltage regulation is given as follows:

$$\frac{V_{\mathrm{dc}}(s)}{V_{\mathrm{dc}}^*(s)} = \frac{\frac{\sqrt{3}Z_{\mathrm{PF1}}k_p I_c}{\overline{V}_{\mathrm{dc}}C_{\mathrm{dc}}}s + \frac{\sqrt{3}Z_{\mathrm{PF1}}k_i I_c}{\overline{V}_{\mathrm{dc}}C_{\mathrm{dc}}}}{s^2 + \frac{\sqrt{3}Z_{\mathrm{PF1}}k_p I_c}{\overline{V}_{\mathrm{dc}}C_{\mathrm{dc}}}s + \frac{\sqrt{3}Z_{\mathrm{PF1}}k_i I_c}{\overline{V}_{\mathrm{dc}}C_{\mathrm{dc}}}}$$
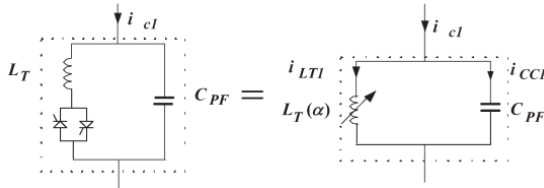
Fig.4.TCR equivalent circuit.

IV. MODELING OF TCR

Fig.4. shows the TCR equivalent circuit. Using Kirchhoff's voltage law, the following equations in 123 reference frame are obtained:

$$v_{s1} = L_T\frac{di_{\mathrm{LT1}}}{dt} + L_{\mathrm{PF}}\frac{di_{c1}}{dt} + R_{\mathrm{PF}}i_{c1} + d_{n1}v_{\mathrm{dc}}$$

$$v_{s2} = L_T\frac{di_{\mathrm{LPF2}}}{dt} + L_{\mathrm{PF}}\frac{di_{c2}}{dt} + R_{\mathrm{PF}}i_{c2} + d_{n2}v_{\mathrm{dc}}$$

$$v_{s3} = L_T\frac{di_{\mathrm{LPF3}}}{dt} + L_{\mathrm{PF}}\frac{di_{c3}}{dt} + R_{\mathrm{PF}}i_{c3} + d_{n3}v_{\mathrm{dc}}$$

$$(19)$$

Applying Park's transformation, one obtains

$$L_T(\alpha)\frac{di_{\mathrm{LTd}}}{dt} = L_T(\alpha)\omega i_{\mathrm{LTq}} + L_{\mathrm{PF}}\omega i_q - L_{\mathrm{PF}}\frac{di_d}{dt} - R_{\mathrm{PF}}i_d - d_{\mathrm{nd}}v_{\mathrm{dc}} + v_d$$

$$L_T(\alpha)\frac{di_{\mathrm{LTq}}}{dt} = -L_T(\alpha)\omega i_{\mathrm{LTd}} - L_{\mathrm{PF}}\omega i_d - L_{\mathrm{PF}}\frac{di_q}{dt} - R_{\mathrm{PF}}i_q - d_{\mathrm{nq}}v_{\mathrm{dc}} + v_q.$$

$$(20)$$

The reactive part is chosen to control the reactive current so that $v_q = 0$ and $L_f(\alpha)\omega i_{\mathrm{LTd}} = 0$

$$\frac{di_{\mathrm{LTq}}}{dt} = B(\alpha)\omega\left[-L_{\mathrm{PF}}\omega i_d - L_{\mathrm{PF}}\frac{di_q}{dt} - R_{\mathrm{PF}}i_q - d_{\mathrm{nq}}v_{\mathrm{dc}}\right]$$

$$(21)$$

Where $B(\alpha)=1/LF(\alpha)\omega$ is the susceptance. An equivalent input u_{qT} is defined as

$$u_{\mathrm{qT}} = \frac{di_{\mathrm{LTq}}}{dt}.$$

$$(22)$$

According to this expression, one deduces

$$B(\alpha)=\frac{u_{\mathrm{qT}}}{\omega\left[-L_{\mathrm{PF}}\omega i_d - L_{\mathrm{PF}}\frac{di_q}{dt} - R_{\mathrm{PF}}i_q - d_{\mathrm{nq}}v_{\mathrm{dc}}\right]}.$$

$$(23)$$

On the other hand, the equivalent inductance is given by

$$L_{\mathrm{PF}}(\alpha) = L_{\mathrm{PF}}\frac{\pi}{2\pi - 2\alpha + \sin(2\alpha)}.$$

$$(24)$$

The susceptance is given by

$$B(\alpha) = B \frac{2\pi - 2\alpha + \sin(2\alpha)}{\pi} \qquad (25)$$

V.FUZZY LOGIC CONTROL

L. A. Zadeh presented the first paper on fuzzy set theory in 1965. Since then, a new language was developed to describe the fuzzy properties of reality, which are very difficult and sometime even impossible to be described using conventional methods. Fuzzy set theory has been widely used in the control area with some application to power system [5]. A simple fuzzy logic control is built up by a group of rules based on the human knowledge of system behaviour. Matlab/Simulink simulation model is built to study the dynamic behaviour of converter. Furthermore, design of fuzzy logic controller can provide desirable both small signal and large signal dynamic performance at same time, which is not possible with linear control technique. Thus, fuzzy logic controller has been potential ability to improve the robustness of compensator.

The basic scheme of a fuzzy logic controller is shown in Fig 5 and consists of four principal components such as: a fuzzy fication interface, which converts input data into suitable linguistic values; a knowledge base, which consists of a data base with the necessary linguistic definitions and the control rule set; a decision-making logic which, simulating a human decision process, infer the fuzzy control action from the knowledge of the control rules and linguistic variable definitions; a de-fuzzification interface which yields non fuzzy control action from an inferred fuzzy control action [10].
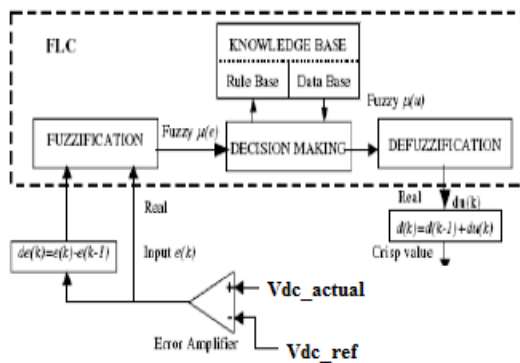
Fig.5. Block diagram of the Fuzzy Logic Controller (FLC) for proposed converter.
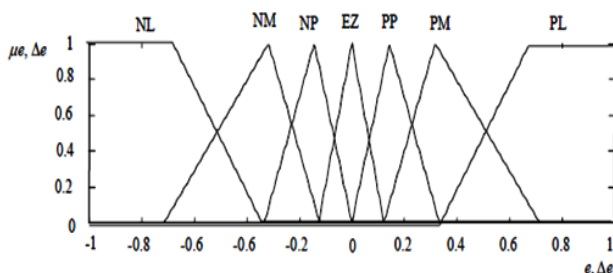
Fig.6. Membership functions for Input, Change in input, Output.

Rule Base: the elements of this rule base table are determined based on the theory that in the transient state, large errors need coarse control, which requires coarse in-put/output variables; in the steady state, small errors need fine control, which requires fine input/output variables. Based on this the elements of the rule table are obtained as shown in Table, with 'Vdc' and 'Vdc-ref' as inputs

$\frac{e}{\Delta e}$	NL	NM	NS	EZ	PS	PM	PL
NL	NL	NL	NL	NL	NM	NS	EZ
NM	NL	NL	NL	NM	NS	EZ	PS
NS	NL	NL	NM	NS	EZ	PS	PM
EZ	NL	NM	NS	EZ	PS	PM	PL
PS	NM	NS	EZ	PS	PM	PL	PL
PM	NS	EZ	PS	PM	PL	PL	PL
PL	NL	NM	NS	EZ	PS	PM	PL

VI.MATLAB/SIMULINK RESULTS

Case 1: Performance of SHPF-TCR for harmonic generated load.
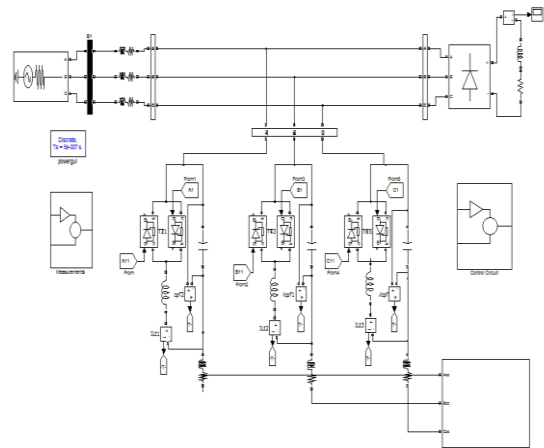
Fig.7.Simulink Circuit for SHPF-TCR under Harmonic Generated Load.
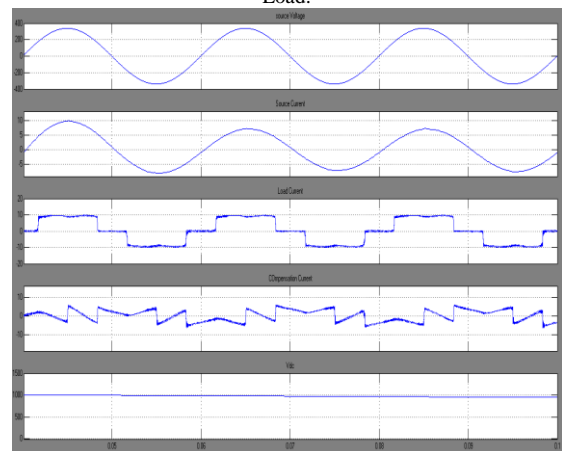
Fig.8.Simulation Results for Source Voltage, Source Current, Load Current, Compensation Currents and Dc Link Voltage.
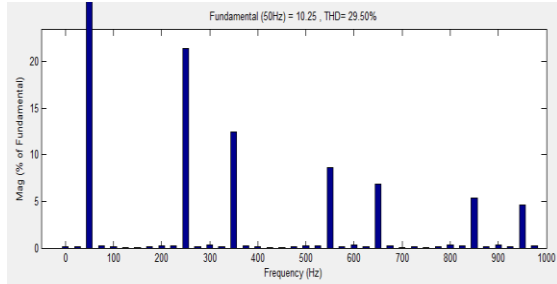
Fig.9.Harmonic Spectrum for Source Current without Compensation.
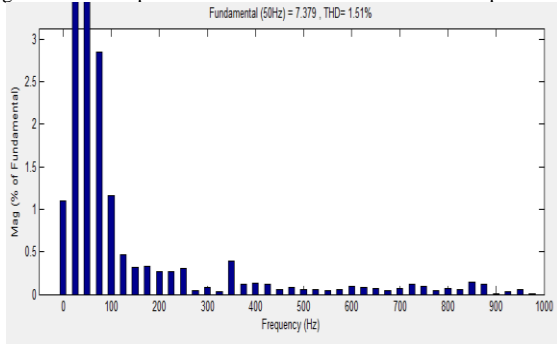
Fig.10.Harmonic Spectrum for Source Current with Compensation.

Case 2: Performance of SHPF-TCR for distorted harmonic generated load
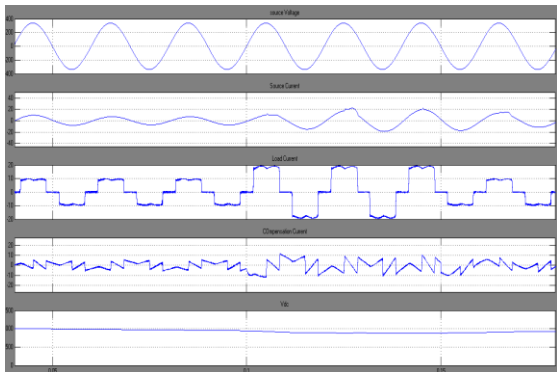
Fig.11.Simulation Results for Source Voltage, Source Current, Load Current, Compensation Currents and Dc Link Voltage
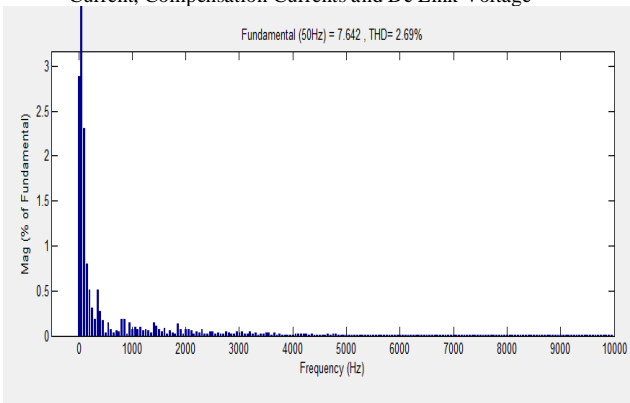
Fig.12.Harmonic Spectrum for Source Current With Compensation.

Case 3: Performance of SHPF-TCR for harmonic and reactive type load
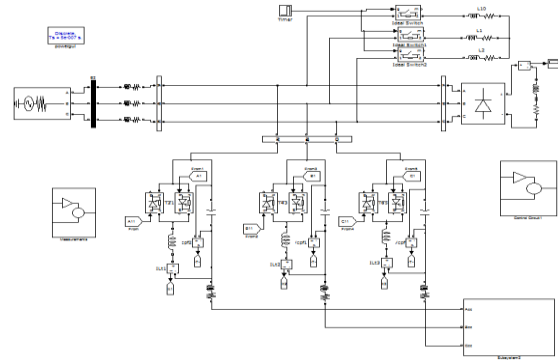
Fig.13.Simulink Circuit for SHAF-TCR for Harmonic and Reactive Type Load.
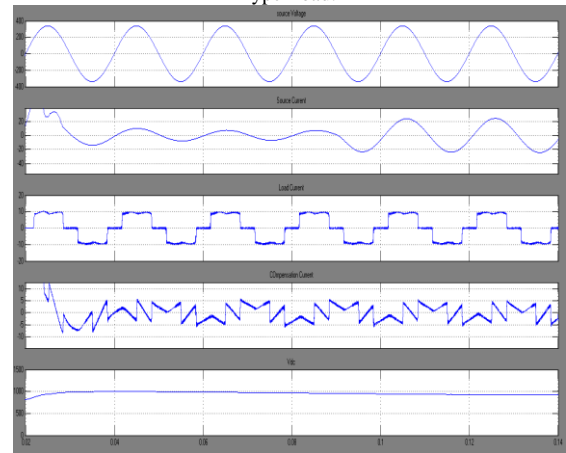
Fig.14.Simulation Results for Source Voltage, Source Current, Load Current, Compensation Currents and Dc Link Voltage
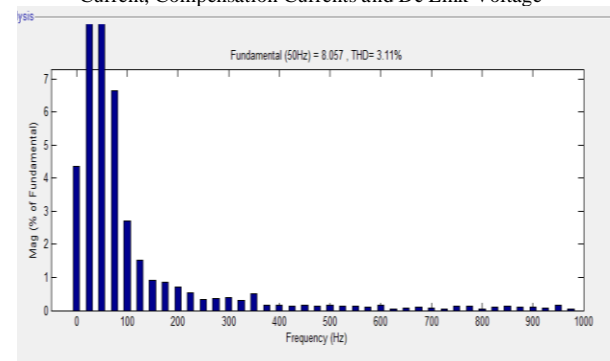
Fig.15.Harmonic Spectrum for Source Current With Compensation.

Case 4: Performance of SHPF-TCR for harmonic generated load with fuzzy controller
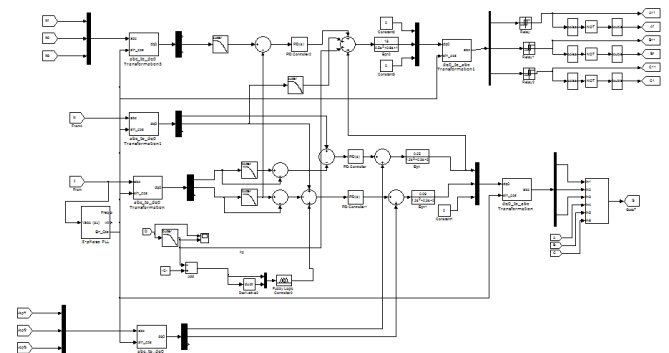
Fig.16.Control Design for Fuzzy Logic Model.
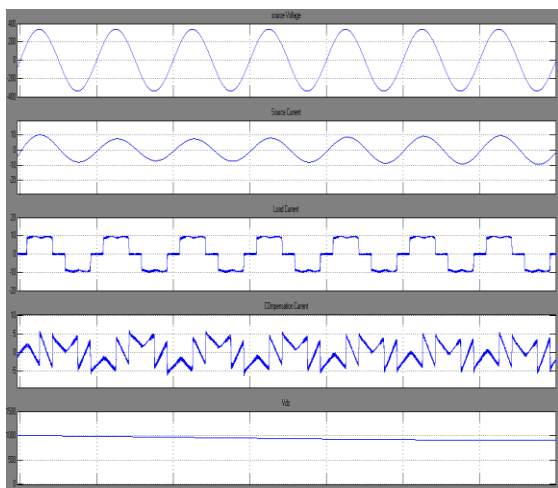
Fig.17.Simulation Results for Source Voltage, Source Current, Load Current, Compensation Currents and Dc Link Voltage.
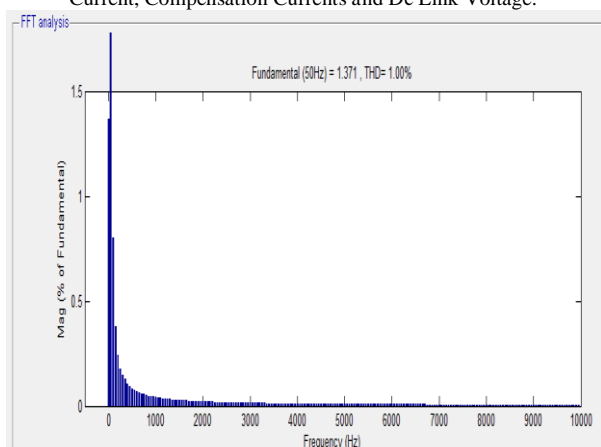
Fig.18.Harmonic Spectrum for Source Current with Compensation.

VII. CONCLUSION

A fuzzy logic HAPF controller has been designed for stabilization of power systems. The control has been tested on several load conditions with transient/dynamic/steady state conditions. The transient response of the power system with the proposed fuzzy controller has been compared with a conventional PI control design. In this paper, a Intelligent based SHPF-TCR compensator of a TCR and a SHPF has been proposed to achieve harmonic elimination and reactive power compensation .The shunt active filter and SPF have a complementary function to improve the performance of filtering and to reduce the power rating requirements of an active filter. The scheme has the advantage of simplicity and is able to provide self-supported dc bus of the active filter through power transfer from ac line at fundamental frequency. The performance of conventional PI controller and fuzzy controller has been studied and compared. Overall, the fuzzy controller gives the best SAPF performance in comparison with the PI controller in regards voltage regulation, % THD, settling time, current overshoot etc.

REFERENCES

[1] A. Hamadi, S. Rahmani, and K. Al-Haddad, "A hybrid passive filter configuration for VAR control and harmonic compensation," IEEE Trans. Ind. Electron., vol. 57, no. 7, pp. 2419–2434, Jul. 2010.

[2] P. Flores, J. Dixon, M. Ortuzar, R. Carmi, P. Barriuso, and L. Moran, "Static Var compensator and active power filter with power injection capability, using 27-level inverters and photovoltaic cells," IEEE Trans.Ind. Electron., vol. 56, no. 1, pp. 130–138, Jan. 2009.

[3] X. Wang, F. Zhuo, J. Li, L. Wang, and S. Ni, "Modeling and control of dual-stage high-power multifunctional PV system in d-q-0 coordinate," IEEE Trans. Ind. Electron., vol. 60, no. 4, pp. 1556–1570, Apr. 2013.

[4] J. A. Munoz, J. R. Espinoza, C. R. Baier, L. A. Moran, E. E. Espinosa, P. E. Melin, and D. G. Sbarbaro, "Design of a discrete-time linear control strategy for a multicell UPQC," IEEE Trans. Ind. Electron., vol. 59, no. 10, pp. 3797–3807, Oct. 2012.

[5] L. Junyi, P. Zanchetta, M. Degano, and E. Lavopa, "Control design and implementation for high performance shunt active filters in aircraft power grids," IEEE Trans. Ind. Electron., vol. 59, no. 9, pp. 3604–3613, Sep. 2012.

[6] Z. Chen, Y. Luo, and M. Chen, "Control and performance of a cascaded shunt active power filter for aircraft electric power system," IEEE Trans. Ind. Electron., vol. 59, no. 9, pp. 3614–3623, Sep. 2012.

[7] S. Rahmani, A. Hamadi, K. Al-Haddad, and A. I. Alolah, "A DSP-based implementation of an instantaneous current control for a three-phase shunt hybrid power filter," J. Math. Comput. Simul.—Model. Simul. Elect. Mach., Convert. Syst., vol. 91, pp. 229–248, May 2013.

[8] A. Hamadi, S. Rahmani, and K. Al-Haddad, "Digital control of hybrid power filter adopting nonlinear control approach," IEEE Trans. Ind. Informat., to be published.

[9] A. Bhattacharya, C. Chakraborty, and S. Bhattacharya, "Parallelconnected shunt hybrid active power filters operating at different

switching frequencies for improved performance," IEEE Trans. Ind. Electron., vol. 59, no. 11, pp. 4007–4019, Nov. 2012.

[10] S. Rahmani, A. Hamadi, N. Mendalek, and K. Al-Haddad, "A new control technique for three-phase shunt hybrid power filter," IEEE Trans. Ind. Electron., vol. 56, no. 8, pp. 2904–2915, Aug. 2009.

[11] A. Luo, X. Xu, L. Fang, H. Fang, J. Wu, and C. Wu, "Feedbackfeedforward PI-type iterative learning control strategy for hybrid active power filter with injection circuit," IEEE Trans. Ind. Electron., vol. 57, no. 11, pp. 3767–3779, Nov. 2010.

[12] M. I. Milanés-Montero, E. Romero-Cadaval, and F. Barrero-González, "Hybrid multiconverter conditioner topology for high-power applications," IEEE Trans. Ind. Electron., vol. 58, no. 6, pp. 2283–2292, Jun. 2011.

[13] A. Luo, S. Peng, C. Wu, J. Wu, and Z. Shuai, "Power electronic hybrid system for load balancing compensation and frequency-selective harmonic suppression," IEEE Trans. Ind. Electron., vol. 59, no. 2, pp. 723– 732, Feb. 2012.

[14] A. Luo, Z. Shuai, W. Zhu, and Z. John Shen, "Combined system for harmonic suppression and reactive power compensation," IEEE Trans. Ind. Electron., vol. 56, no. 2, pp. 418–428, Feb. 2009.